# Kinetics of Spiro Meisenheimer Complex Formation from 3,6-Dimethylcatechol 2,4,6-Trinitrophenyl Ether. Competition between a Trapping and a Preassociation Mechanism[1]

**Claude F. Bernasconi* and Douglas E. Fairchild**

*Contribution from the Thimann Laboratories of the University of California, Santa Cruz, California 95064.* *Received November 12, 1987. Revised Manuscript Received March 28, 1988*

**Abstract:** The ionized form of catechol 2,4,6-trinitrophenyl ether was reported in 1976 to cyclize and form a spiro Meisenheimer complex with a rate constant in the order of $10^9$ $s^{-1}$ in 50% $Me_2SO$–50% water. A stopped-flow and temperature-jump study of the cyclization of 3,6-dimethylcatechol 2,4,6-trinitrophenyl ether in the same solvent reported in this paper shows that the two methyl groups enhance the intramolecular nucleophilic addition rate still further. The results are consistent with the operation of two competing mechanisms: the first is a trapping mechanism that involves diffusion-controlled proton transfer between the phenolic hydroxyl and carboxylate ions and cyclization/ring opening occurring in the absence of catalysts; the second is a preassociation mechanism in which the cyclization/ring opening step involves buffer catalysis by hydrogen bonding. A reanalysis of the 1976 data for catechol 2,4,6-trinitrophenyl ether suggests that there is also a contribution by the preassociation mechanism but a very small one. The increase in the cyclization rate by the methyl groups in the 3,6-dimethylcatechol moiety is explained in terms of a steric effect that enhances the population of a more reactive conformation. This explanation is the same as that offered by Bunnett and Okamoto for the acceleration of the Smiles rearrangement of 2-hydroxy-2′-nitrodiphenyl sulfone to 2-(*o*-nitrophenoxy)benzenesulfinic acid, although the rate enhancement observed in the present work is much less dramatic than in the Smiles rearrangement.

In 1976 we reported a temperature-jump kinetic study of spiro Meisenheimer complex formation from catechol 2,4,6-trinitrophenyl ether (**1**) in 50% $Me_2SO$–50% water (v/v),[2] (eq 1).

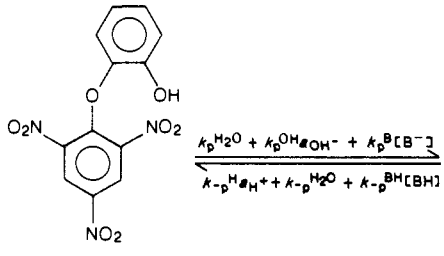

**1**

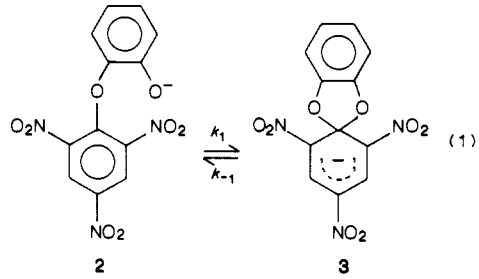

(1)

**2** **3**

One of the most remarkable findings of this study was that deprotonation of **1** is rate limiting at low carboxylic acid (BH) buffer concentrations while $k_1$ becomes partially corate limiting at high buffer concentrations. This implies a very high rate for the cyclization step; assuming that the proton-transfer step is diffusion controlled, a $k_1 \approx 1.2 \times 10^9$ $s^{-1}$ was calculated.

As high as this $k_1$ value appears to be, we became intrigued by the possibility of enhancing it further, perhaps to a point that would make the lifetime of **2** so short as to enforce a change in the mechanism of reaction. For example, a relatively modest increase in $k_1$ to say $10^{10}$ or $10^{11}$ $s^{-1}$ would make the cyclization competitive with diffusional separation of BH from **2**. In such a case intramolecular attack would precede this diffusional separation, and the ring *opening* reaction (reverse direction) would have to occur after a preassociation equilibrium between the spiro complex **3** and BH, as shown in eq 2. This is known as a preassociation mechanism.[3]

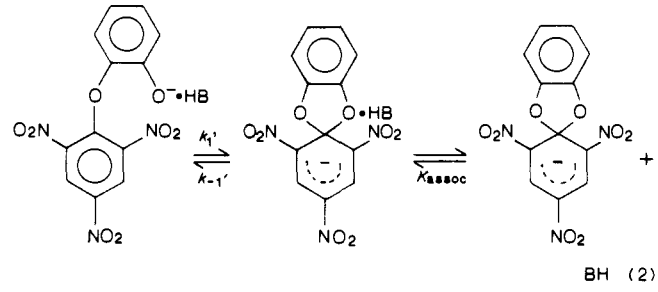

BH (2)

If $k_1$ could be pushed to a value $>10^{13}$ $s^{-1}$, which would reduce the lifetime of **2** below that of a molecular vibration, **2** could no longer exist as an intermediate. In such a case the reaction would become enforced concerted[3] and proceed as shown in eq 3.

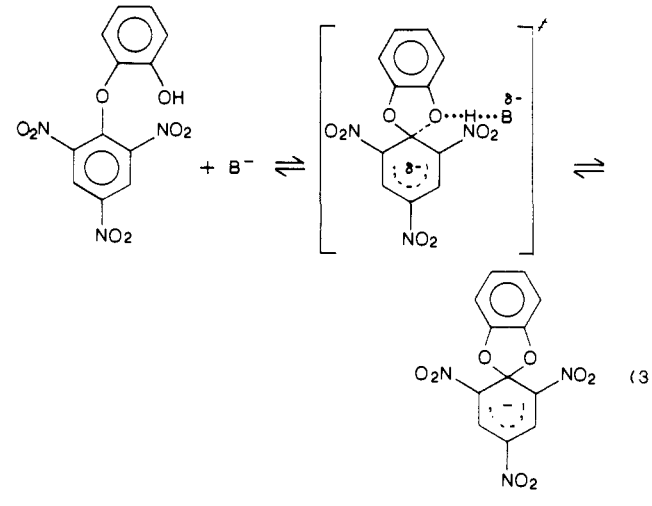

(3)

A possible method for enhancing $k_1$ substantially and perhaps dramatically suggested itself on the basis of the work of Bunnett and Okamoto.[4] These authors reported rate accelerations in the

(1) This is part 23 in the series "Intermediates in Nucleophilic Aromatic Substitution". Part 22: Bernasconi, C. F.; Howard, K. A. *J. Am. Chem. Soc.* **1983**, *105*, 4690.

(2) Bernasconi, C. F.; Wang, H.-C. *J. Am. Chem. Soc.* **1976**, *98*, 6265.

(3) (a) Jencks, W. P. *Chem. Soc. Rev.* **1981**, *10*, 345. (b) Jencks, W. P. *Acc. Chem. Res.* **1980**, *13*, 161.

(4) Bunnett, J. F.; Okamoto, T. *J. Am. Chem. Soc.* **1956**, *78*, 5363.

0002-7863/88/1510-5498$01.50/0 

order of 500 000-fold for the Smiles rearrangement of eq 4 when

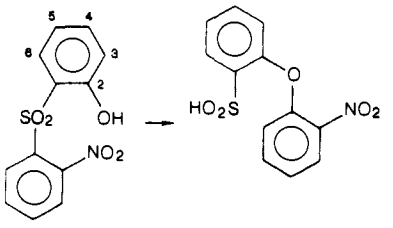

(4)

**4**

a substituent such as methyl, bromo or chloro was introduced into the 6-position of the phenolic benzene ring. This acceleration was attributed to a steric regulation of rotational conformation, which can be visualized as follows. According to Bunnett and Okamoto the preferred conformation of the unsubstituted substrate is **4a**; c indicates the activated benzene ring, which is perpendicular to the plane of the paper. The more reactive conformation **4b** in

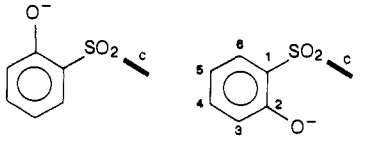

**4a** **4b**

which the nucleophilic oxygen is optimally positioned for attack at the 1-position of the c ring is disfavored because of steric repulsion between $O^-$ and the c ring. Introduction of a 6-substituent that is bulkier than $O^-$ renders **4b** more favorable, however. Hence the accelerating effect of the 6-substituent can be understood as the consequence of locking the substrate into its more reactive conformation **4b**.

By applying the same reasoning to **2**, it would appear that **2a** is the most stable conformation while **2b** should be the most reactive one. Locking the anion of catechol 2,4,6-trinitrophenyl ether into the **2a** conformation by introducing a substituent into the 6-position should then enhance $k_1$ in a similar way as the 6-substituents in **4** enhance the Smiles rearrangement.

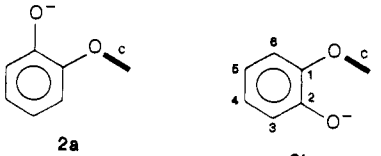

**2a** **2b**

In this paper we report results of a test of this hypothesis. Because reaction 1 is reversible it seemed advisable to use a symmetrically substituted catechol derivative. We chose the 3,6-dimethylcatechol 2,4,6-trinitrophenyl ether, **5**, for this purpose. We did observe an increase in $k_1$, but it is not nearly as dramatic as the one reported by Bunnett and Okamoto.

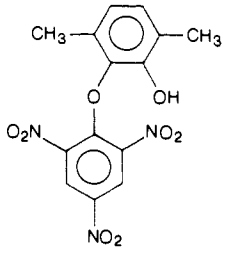

(5)

**5**

## Results

**General Features.** The results to be presented are, in broad terms, consistent with the two-step mechanism discussed previously for the parent catechol 2,4,6-trinitrophenyl ether (eq 1). It can be schematically represented by

$$SH \underset{k_{-p}}{\overset{k_p}{\rightleftharpoons}} S^- \underset{k_{-1}}{\overset{k_1}{\rightleftharpoons}} M^- \qquad (6)$$

**Table I.** Equilibrium Constant as Function of Buffer Concentration at $[BH]_o \geq 0.1$ M

| $[BH]_o$, M | $10^4[SH]_o$, M | OD | $10^5K_o$, M | $pK_o$ |
|---|---|---|---|---|
| A. Chloroacetic Acid, pH 3.71, $[BH]:[B^-] = 1:1$ | | | | |
| 0.2 | 0.686 | 0.411 | 9.18 | 4.03 |
| 0.4 | 0.686 | 0.436 | 10.04 | 4.00 |
| 0.6 | 0.686 | 0.459 | 10.88 | 3.97 |
| 0.8 | 0.686 | 0.470 | 11.29 | 3.95 |
| 1.0 | 0.686 | 0.483 | 11.80 | 3.92 |
| B. Methoxyacetic Acid, pH 2.97, $[BH]:[B^-] = 39:1$ | | | | |
| 0.1 | 5.47 | 0.784 | 8.47 | 4.08 |
| 0.2 | 4.25 | 0.651 | 9.15 | 4.04 |
| 0.3 | 5.47 | 0.879 | 9.66 | 4.02 |
| 0.4 | 4.25 | 0.718 | 10.24 | 3.99 |
| 0.5 | 5.47 | 0.962 | 10.72 | 3.96 |
| 0.6 | 4.25 | 0.793 | 11.48 | 3.94 |
| 0.7 | 5.47 | 1.066 | 12.07 | 3.91 |
| 0.8 | 4.25 | 0.884 | 13.03 | 3.89 |
| 0.9 | 4.25 | 0.894 | 13.20 | 3.87 |
| 1.0 | 4.25 | 0.955 | 14.26 | 3.85 |

with SH = **5** and $M^-$ being the corresponding Meisenheimer complex. $k_p$ and $k_{-p}$ are defined as

$$k_p = k_p^{H_2O} + k_p^{OH}a_{OH^-} + k_p^{B}[B^-] \qquad (7)$$

$$k_{-p} = k_{-p}^{H}a_{H^+} + k_{-p}^{H_2O} + k_{-p}^{BH}[BH] \qquad (8)$$

Our initial analysis of the kinetic results will be based on this mechanism. However, in the Discussion section it will be shown that there is some competition by a preassociation mechanism. This will require some modification of the analysis.

Since no kinetic measurements above pH 6.38 were performed, the $k_p^{OH}a_{OH^-}$ (eq 7) and $k_{-p}^{H_2O}$ (eq 8) terms were always negligible. For the same reason, $S^-$ never accumulates to measurable concentrations (pH $\ll pK_a^{OH}$ with $pK_a^{OH}$ being the $pK_a$ of SH). This means that $S^-$ can be treated as a steady-state intermediate, and thus the reciprocal relaxation time for equilibrium approach is given by

$$\tau^{-1} = \frac{k_pk_1}{k_{-p} + k_1} + \frac{k_{-p}k_{-1}}{k_{-p} + k_1} \qquad (9)$$

All rate and equilibrium measurements were made in 50% $Me_2SO$–50% water at 20 °C, at a constant ionic strength of 0.5 M maintained with KCl. Rates were measured in acetate, methoxyacetate, chloroacetate, and dichloroacetate buffers. Pseudo-first-order conditions were used throughout. At low buffer concentrations the rates were slow enough to be measured in the stopped-flow apparatus; at high buffer concentrations the temperature-jump technique had to be used. In the region of overlap of the two techniques, excellent agreement was found between the results from the two methods.

**Equilibrium Measurements.** One may define an apparent equilibrium constant, $K_o = K_a^{OH}K_1$ referring to the overall reaction $SH \rightleftarrows M^- + H^+$, with $K_1$ being the equilibrium constant for cyclization and $K_a^{OH}$ the acid dissociation constant of SH. The strong absorption of the spiro complex at 472 nm could easily be exploited for a spectrophotometric determination of $K_o$. A $K_o = (9.12 \pm 0.10) \times 10^{-5}$ M ($pK_o = 4.04$) was found in *dilute* buffer solutions.

In order to test whether the high buffer concentrations used in some of the kinetic experiments described below may affect $K_o$ by a salt or medium effect, equilibrium absorbances were determined under the same conditions as for these kinetic experiments. The results of these determinations are summarized in Table I. They show that $K_o$ increases ($pK_o$ decreases) somewhat with increasing chloroacetic and methoxyacetic acid buffer concentration.

**Kinetics at Low Buffer Concentrations (Stopped-Flow Experiments).** $\tau^{-1}$ was determined in acetate (pH 6.38 and 5.78), methoxyacetate (pH 5.16 and 4.56), chloroacetate (pH 4.31 and 3.71), and dichloroacetate (pH 3.10, 2.75 and 2.15) buffers. At any given pH, $\tau^{-1}$ was typically obtained at 8–13 different buffer

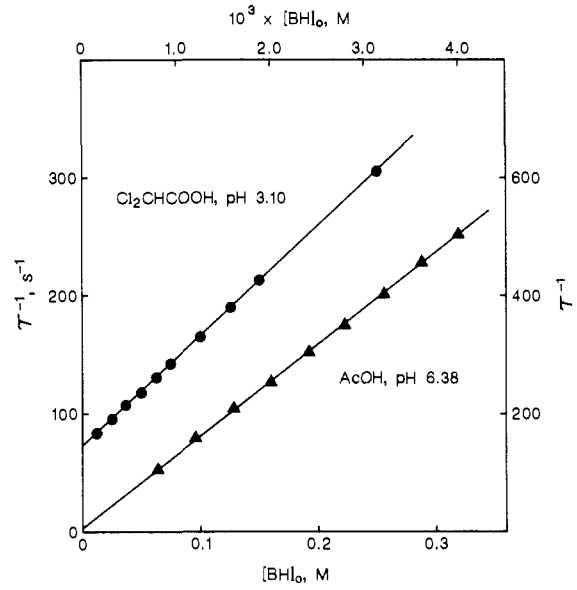


**Figure 1.** Representative plots of $\tau^{-1}$ vs total buffer concentration, stopped flow data. Circles: $Cl_2CHCOOH$, left $y$ axis, bottom $x$ axis. Triangles: AcOH, right $y$ axis, top $x$ axis.

**Table II.** Slopes and Intercepts of Buffer Plots, Analysis According to Eq 10

| buffer | pH | intercept,[b] $s^{-1}$ | $10^{-3}$ × slope$(K_a^{BH} + a_{H^+})/a_{H^+}$,[c] $M^{-1}$ $s^{-1}$ |
|---|---|---|---|
| $Cl_2CHCOOH$ | 2.15 | 510 ± 5 | 8 ± 2 |
| | 2.75 | 160 ± 2 | 8.63 ± 0.04 |
| | 3.10 | 72 ± 1 | 9.36 ± 0.15 |
| $ClCH_2COOH$ | 3.71 | 25 ± 2 | 7.23 ± 0.03 |
| | 4.31 | 11.1 ± 0.8 | 14.48 ± 0.06 |
| $CH_3OCH_2COOH$ | 4.56 | 10.2 ± 1.3 | 16.1 ± 0.3 |
| | 5.16 | 6.6 ± 2.2 | 52.0 ± 0.3 |
| $CH_3COOH$ | 5.78 | *a* | 162 ± 3 |
| | 6.38 | *a* | 631 ± 11 |

[a] Too small to measure accurately. [b] Intercept = $k_p^{H_2O} + (k_{-p}^{H}/K_1)a_{H^+}$. [c] Slope $(K_a^{BH} + a_{H^+})/a_{H^+} = (k_p^{B}K_a^{BH}/a_{H^+}) + (k_{-p}^{BH}/K_1)$.

concentrations. The results are summarized in Tables S1–S4[5] (90 $\tau^{-1}$ values). Figure 1 shows some representative plots of $\tau^{-1}$ vs total acetic acid and dichloroacetic acid concentration. The linearity of the plots implies that $k_1 \gg k_{-p}$, which reduces eq 9 to

$$\tau_{low}^{-1} = k_p + k_{-p}/K_1 = k_p^{H_2O} + \frac{k_{-p}^{H}}{K_1}a_{H^+} + \left(k_p^{B}\frac{K_a^{BH}}{a_{H^+}} + \frac{k_{-p}^{BH}}{K_1}\right)\frac{a_{H^+}}{K_a^{BH} + a_{H^+}}[BH]_o \quad (10)$$

with $K_a^{BH}$ being the acid dissociation constant of the buffer. The slope × $(K_a^{BH} + a_{H^+})/a_{H^+}$ and intercepts of these plots are summarized in Table II. From a plot (not shown) of the intercepts vs $a_{H^+}$, one obtains $k_p^{H_2O} = 6.76 \pm 0.73$ $s^{-1}$ and $k_{-p}^{H}/K_1 = (8.56 \pm 0.10) \times 10^4$ $M^{-1}$ $s^{-1}$. The ratio $k_p^{H_2O}(k_{-p}^{H}/K_1) = K_a^{OH}K_1 = K_o = (7.9 \pm 1.0) \times 10^{-5}$ M is in good agreement with the spectrophotometric $K_o = (9.12 \pm 0.10) \times 10^{-5}$ M.

By plotting the slopes × $(K_a^{BH} + a_{H^+})/a_{H^+}$ vs $K_a^{BH}/a_{H^+}$ (not shown), values for $k_p^{B}$ and $k_{-p}^{BH}/K_1$ could be obtained. For the acetate and methoxyacetate buffers, $k_p^{B}K_a^{BH}/a_{H^+} \gg k_{-p}^{BH}/K_1$ so the slopes only provide $k_p^{B}$ while $k_{-p}^{BH}/K_1$ was then calculated by using the known value of $K_o$ (since $k_p^{B}/k_{-p}^{BH} = K_o/K_a^{BH}$). At the other extreme, with the dichloroacetate buffer, $k_p^{B}K_a^{BH}/a_{H^+} \ll k_{-p}^{BH}/K_1$ and the slopes only afford a reliable value for $k_{-p}^{BH}/K_1$; in this case $k_p^{B}$ is calculated with the help of $K_o$. The results of this analysis are summarized in Table III.

(5) See paragraph concerning supplementary material at the end of this paper.

**Table III.** Analysis of Slopes and Intercepts from Table II

| BH | $pK_a^{BH}$ | $k_p^{B}$, $M^{-1}$ $s^{-1}$ | $k_{-p}^{BH}/K_1$, $M^{-1}$ $s^{-1}$ |
|---|---|---|---|
| $H_3O^+$ | −1.44 | 6.76 ± 0.73[a] | (8.56 ± 0.10) × $10^4$ |
| $Cl_2CHCOOH$ | 2.15 | (1.04 ± 0.08) × $10^2$ | (8.04 ± 0.20) × $10^3$ |
| $ClCH_2COOH$ | 3.71 | (2.43 ± 0.03) × $10^3$ | (4.79 ± 0.07) × $10^3$ |
| $CH_3OCH_2COOH$ | 4.56 | (1.20 ± 0.02) × $10^4$ | (3.62 ± 0.24) × $10^3$ |
| $CH_3COOH$ | 5.78 | (1.57 ± 0.05) × $10^5$ | (2.86 ± 0.23) × $10^3$ |

[a] Units = $s^{-1}$.

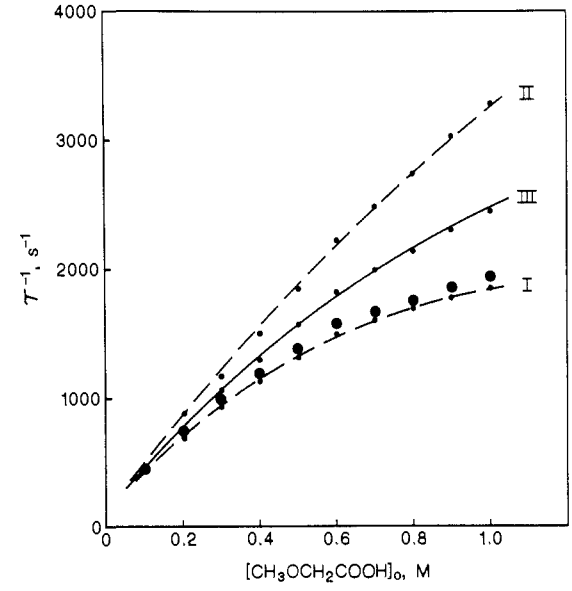


**Figure 2.** $\tau^{-1}$ from temperature-jump experiments in methoxyacetic acid buffers at pH 2.97. Large points are experimental values. Small points represent $\tau^{-1}$ values corrected for medium effect according to the cases I–III discussed in the text. Case III is the preferred one.

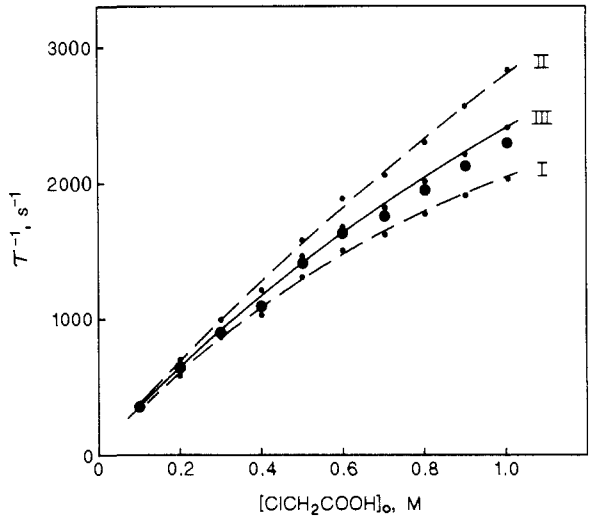


**Figure 3.** $\tau^{-1}$ from temperature-jump experiments in chloroacetic acid buffers at pH 3.71. Large points are experimental values. Small points represent $\tau^{-1}$ values corrected for medium effect according to the cases I–III discussed in the text. Case III is the preferred one.

**Kinetics of High Buffer Concentrations (Temperature-Jump Experiments).** Temperature-jump experiments in chloroacetate (pH 3.71) and methoxyacetate (pH 2.97) buffers at concentrations up to 1 M total buffer concentration were performed in order to explore whether $k_1$ and $k_{-1}$ might become co-rate-limiting with proton transfer due to a change from $k_1 \gg k_{-p}$ to $k_1 \lesssim k_{-p}$ at high concentrations. The results are summarized in Table S5[5] while Figures 2 and 3 show plots of $\tau^{-1}$ vs total buffer concentration. The plots are curved, which is consistent with $k_{-p}$ becoming comparable to $k_1$.

**Table IV.** Analysis of Results at High Buffer Concentration

| | $ClCH_2COOH$ | $CH_3OCH_2COOH$ |
|---|---|---|
| A. Analysis before Correction for Medium Effect | | |
| $k_1/k_{-p}^{BH}$, M[a] | 1.08 ± 0.10 | 0.763 ± 0.026 |
| $\tau_{hi}^{-1}$, $s^{-1}$ [a] | (7.24 ± 0.60) × $10^3$ | (3.44 ± 0.08) × $10^3$ |
| $k_1$, $s^{-1}$ [b] | (1.08 ± 0.10) × $10^{10}$ | (7.63 ± 0.26) × $10^9$ |
| $k_1K_a^{OH}$, M $s^{-1}$ [c] | 0.90 ± 0.15 | |
| $pK_a^{OH}$ [d] | 10.08 ± 0.12 | 9.93 ± 0.09 |
| $k_{-1}$, $s^{-1}$ [c] | (2.61 ± 0.07) × $10^3$ | |
| $K_1$ [e] | 4.14 × $10^6$ | 2.92 × $10^6$ |
| $pK_o$ [f] | 3.46 ± 0.08 | |
| B. Analysis after Correction for Medium Effect (Case III) | | |
| $k_1/k_{-p}^{BH}$, M[a] | 1.28 ± 0.13 | 1.28 ± 0.05 |
| $\tau_{hi}^{-1}$, $s^{-1}$ [a] | (8.62 ± 0.70) × $10^3$ | (5.62 ± 0.16) × $10^3$ |
| $k_1$, $s^{-1}$ [b] | (1.28 ± 0.13) × $10^{10}$ | (1.28 ± 0.05) × $10^{10}$ |
| $k_1K_a^{OH}$, M $s^{-1}$ [c] | 0.71 ± 0.22 | |
| $pK_a^{OH}$ [d] | 10.25 ± 0.16 | 10.25 ± 0.16 |
| $k_{-1}$, $s^{-1}$ [c] | (4.95 ± 0.20) × $10^3$ | |
| $K_1$ [e] | 2.59 × $10^6$ | 2.59 × $10^6$ |
| $pK_o$ [f] | 3.84 ± 0.16 | |

[a] From plots of $\tau$ vs $[BH]^{-1}$ according to eq 12. [b] Calculated from $k_1/k_{-p}^{BH}$ assuming $k_{-p}^{BH} = 10^{10}$ $M^{-1}$ $s^{-1}$. [c] From pH dependence of $\tau_{hi}^{-1}$. [d] From $k_1K_a^{OH}$ and $k_1$ above. [e] From $k_1/k_{-1}$. [f] $K_o = K_a^{OH}k_1/k_{-1}$.

In a first approximation we shall assume that the increase in $k_{-p}$ (eq 9) is the only reason for the curvature in Figures 2 and 3; this assumption will be refined later by considering medium effects as coresponsible for the curvature. Since at high buffer concentrations $k_p \approx k_p^B[B]$ and $k_{-p} \approx k_{-p}^{BH}[BH]$, eq 9 simplifies to

$$\tau^{-1} = \frac{k_1k_p^B[B]}{k_{-p}^{BH}[BH] + k_1} + \frac{k_{-1}k_{-p}^{BH}[BH]}{k_{-p}^{BH}[BH] + k_1} \quad (11)$$

Equation 11 may be transformed[2] into

$$\tau = \tau_{hi} + \tau_{hi}\frac{k_1}{k_{-p}^{BH}[BH]} \quad (12)$$

with

$$\tau_{hi} = \left(\frac{K_a^{OH}k_1}{a_{H^+}} + k_{-1}\right)^{-1} \quad (13)$$

Plots of $\tau$ vs $[BH]^{-1}$ (not shown) are linear. They afford the $k_1/k_{-p}^{BH}$ and $\tau_{hi}^{-1}$ values summarized in Table IV, part A. From the pH-dependence of $\tau_{hi}^{-1}$ one further obtains $K_a^{OH}k_1$ and $k_{-1}$ (also in Table IV). If a value for $k_{-p}^{BH}$, which presumably represents diffusion-controlled proton transfer from BH to the oxyanion in $S^-$, is assumed, $k_1$ can also be calculated. For consistency with our previous study with the parent catechol 2,4,6-trinitrophenyl ether,[2] we have assumed $k_{-p}^{BH} = 10^{10}$ $M^{-1}$ $s^{-1}$ for both chloroacetic and methoxyacetic acid, a point to which we shall return in the Discussion.

**Medium Effect.** If a value for $K_o$ is calculated as $K_a^{OH}k_1/k_{-1}$, one obtains $pK_o = 3.46 \pm 0.08$, which is in rather poor agreement with $pK_o = 4.10$ determined from kinetics at low buffer concentrations, or the spectrophotometric $pK_o = 4.04$, which also refers to dilute buffer solutions. This rather large discrepancy between the results of high and low buffer concentrations can be largely traced to a medium effect that contributes to the downward curvature of the buffer plots in Figures 2 and 3. As the data summarized in Table I show, $K_o$ increases with increasing buffer concentration. It should be noted that the reaction conditions for the $K_o$ measurements in Table I were exactly the same as those for the kinetic experiments in Figures 2 and 3.

There may be a number of causes for this medium effect: buffer association such as $BH{\cdot}B^-$, a differential salt effect due to replacement of $Cl^-$ by a carboxylate ion ($B^-$), and the lowering of the dielectric constant of the solvent upon addition of large amounts of the buffer acid. Since buffer association would probably have little effect on $K_o$, this latter effect may be relatively unimportant. On the other hand, $K_o$ is quite sensitive to changes in the dielectric constant as shown by the large increases in $K_o$ upon addition of 2-methyl-2-butanol (Table V), and hence this effect may very well be the most important one.

**Table V.** Equilibrium Constant as a Function of Concentration of Added 2-Methyl-2-butanol at 20 °C[a]

| [ROH], M | pH | $10^4[SH]_o$, M | OD | $10^5K_o$, M | $pK_o$ |
|---|---|---|---|---|---|
| 0 | 3.12 | 1.59 | 0.313 | 8.63 | 4.06 |
| 0.1 | 3.14 | | 0.388 | 10.60 | 3.97 |
| 0.2 | 3.16 | | 0.490 | 13.40 | 3.87 |
| 0.3 | 3.18 | | 0.605 | 16.66 | 3.78 |
| 0.4 | 3.20 | | 0.758 | 21.42 | 3.67 |
| 0.5 | 3.21 | | 0.905 | 26.85 | 3.57 |
| 0.6 | 3.27 | 0.598 | 0.425 | 33.04 | 3.48 |
| 0.8 | 3.30 | | 0.516 | 43.27 | 3.36 |

[a] In 0.001 M HCl, 50% $Me_2SO$/50% water, $\mu$ = 0.5 M (KCl).

In order to estimate how much of the downward curvature in the buffer plots may be attributable to the medium effect, we performed the following analysis. If eq 6 is written as an overall reaction

$$SH \underset{k_r}{\overset{k_f}{\rightleftharpoons}} M^- + H^+ \quad (14)$$

eq 9 can be expressed as

$$\tau^{-1} = k_f + k_r \quad (15)$$

with $k_f = k_pk_1/(k_{-p} + k_1)$, $k_r = k_{-p}k_{-1}/(k_{-p} + k_1)$, and $k_f/k_r = K_o/a_{H^+}$. One may now calculate the medium effect on $\tau^{-1}$ (for details see the Experimental Section) for three extreme cases as follows. Case I: The entire increase in $K_o$ is due to a corresponding increase in $k_f$ while $k_r$ remains unchanged. Case II: The entire increase in $K_o$ is due to a corresponding decrease in $k_r$ while $k_f$ is constant. Case III: Half of the increase in $K_o$ is caused by an increase in $k_f$, the other half by a decrease in $k_r$. The dashed curves in Figures 2 and 3 show the buffer plots after correction for the medium effect for cases I–III. A recalculation of the various kinetic parameters based on case III gave the most internally consistent set of rate and equilibrium constants (Table IV, part B). Specifically, $k_1$, which was significantly different for the two buffers before the correction, is now seen to be the same, and $pK_o$ is now much closer to the values determined at low buffer concentrations, either kinetically (4.10) or spectrophotometrically (4.04). We shall therefore adopt case III in our subsequent discussion.

## Discussion

**Mechanism.** In the Results section we have analyzed our kinetic data on the basis of the scheme in eq 6. In terms of Jencks'[3] terminology, eq 6 in the reverse direction constitutes a trapping mechanism by diffusion-controlled protonation of the intermediate $S^-$. The most salient feature of our results that supports this mechanism is the downward curvature of the buffer plots at high concentration. This curvature is indicative of a change from rate-limiting proton transfer at low buffer concentration, to (partially) rate-limiting cyclization/ring opening at high concentrations.

A complicating feature in our analysis is a medium effect that contributes to the downward curvature. We have corrected the $\tau^{-1}$ values for this effect by making "reasonable" assumptions that lead to the internally most consistent kinetic and equilibrium parameters, but some room for error remains. It is to be noted, though, that even if one made the most extreme and unrealistic assumptions according to which the observed medium effect on $K_o$ is entirely caused by changes in $k_r$ (case II, see Results section), the plots of $\tau^{-1}$ vs [BH] would still show downward curvature (Figures 2 and 3). Hence the change in rate-limiting step appears to be firmly established, in support of the mechanism of eq 6.

Evidence based on Brønsted plots suggests that there is a competing pathway, though. Figure 4 shows Brønsted plots for $k_p^B$ and $k_{-p}^{BH}/K_1$, kinetic parameters that were obtained at low buffer concentrations. They afford $\beta = 0.87 \pm 0.01$ ($k_p^B$) and

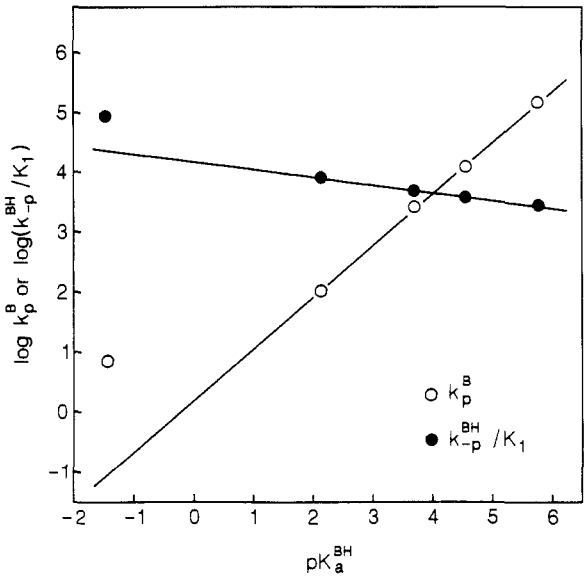


**Figure 4.** Brønsted plots for $k_p^B$ ($\beta = 0.87 \pm 0.01$) and $k_{-p}^{BH}/K_1$ ($\alpha = 0.13 \pm 0.01$).

**Scheme I**

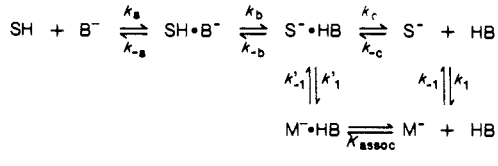


$\alpha = 0.13 \pm 0.01$ ($k_{-p}^{BH}/K_1$). Since the p$K_a$ difference between SH (p$K_a^{OH} \sim 10$) and the buffers (p$K_a^{BH}$ ranges from 2.15 to 5.78) is quite large, one would expect that the proton transfer rates are entirely controlled by diffusion and thus $\beta = 1.0$ and $\alpha = 0.0$.[7,8] The observed $\alpha$ and $\beta$ values are more typical for a preassociation mechanism with weak hydrogen bonding in the transition state.[3]

Scheme I shows such a mechanism, along with the trapping mechanism and a dissection of the Eigen[7] proton-transfer mechanism into its component steps: $k_a$, $k_{-a}$, $k_c$, $k_{-c}$ are diffusional steps, $k_1$ and $k_{-1}$ have the same meaning as in eq 6, $k'_1$ and $k'_{-1}$ are the rate constants for cyclization/ring opening in the presence of an associated buffer acid molecule, while $K_{assoc}$ is the equilibrium constant for the preassociation of $M^-$ with **BH** (eq 2). The pathway $k_a \rightarrow k_b \rightarrow k_c \rightarrow k_1$; $k_{-1} \rightarrow k_{-c} \rightarrow k_{-b} \rightarrow k_{-a}$ is thus the trapping mechanism, the pathway $k_a \rightarrow k_b \rightarrow k'_1$; $K_{assoc} \rightarrow k'_{-1} \rightarrow k_{-b} \rightarrow k_{-a}$ the preassociation mechanism. Note that the global rate constants for the proton transfer in the trapping mechanism are

$$k_p^B = K_a K_b k_c \quad (16)$$

$$k_{-p}^{BH} = k_{-c} \quad (17)$$

with

$$K_a = k_a/k_{-a} \qquad K_b = k_b/k_{-b} \quad (18)$$

The global rate constants for the preassociation mechanism are

$$k_f^{pre} = K_a K_b k'_1 \quad (19)$$

$$k_r^{pre} = K_{assoc} k'_{-1} \quad (20)$$

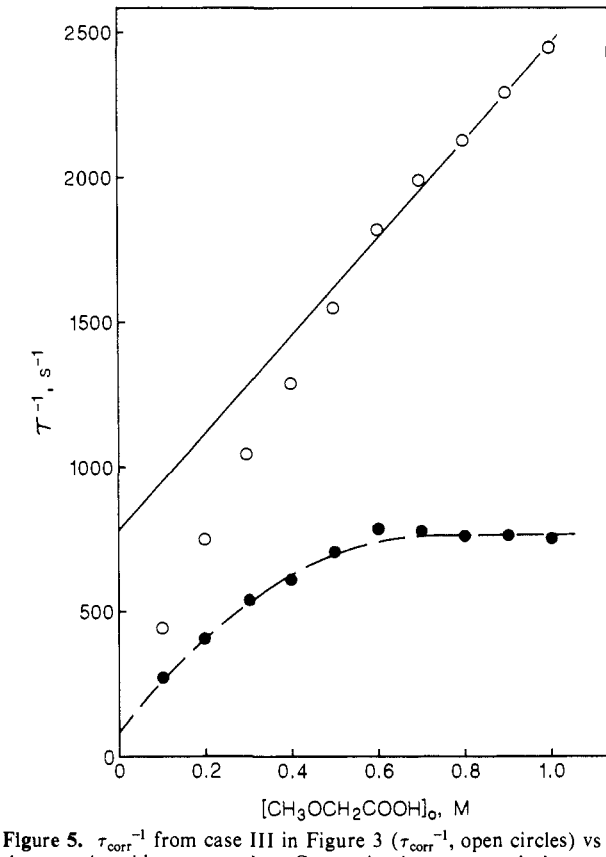


**Figure 5.** $\tau_{corr}^{-1}$ from case III in Figure 3 ($\tau_{corr}^{-1}$, open circles) vs methoxyacetic acid concentration. Separation into preassociation mechanism ($\tau_{pre}^{-1}$, solid line) and trapping mechanism ($\tau_{trap}^{-1}$, filled circles) as discussed in text.

If the two mechanisms compete, eq 9 will contain two additional terms and become

$$\tau^{-1} = \frac{k_1 k_p}{k_{-p} + k_1} + \frac{k_{-1} k_{-p}}{k_{-p} + k_1} + k_f^{pre}[B] + k_r^{pre}[BH] \quad (21)$$

while the limiting case for low buffer concentrations ($k_1 \gg k_{-p}$) is given by

$$\tau_{low}^{-1} = k_p^{H_2O} + \frac{k_{-p}^H}{K_1} a_{H^+} + \left( k_p^B \frac{K_a^{BH}}{a_{H^+}} + \frac{k_{-p}^{BH}}{K_1} + k_f^{pre} \frac{K_a^{BH}}{a_{H^+}} + k_r^{pre} \right) \frac{a_{H^+}}{K_a^{BH} + a_{H^+}} [BH]_o \quad (22)$$

In this case the quantity labeled $k_p^B$ in Table III and on the Brønsted plot (Figure 4) would take on the meaning of $k_p^B + k_f^{pre}$, while the quantity labeled $k_{-p}^{BH}/K_1$ would in fact be $k_{-p}^{BH}/K_1 + k_r^{pre}$.

Inasmuch as there is hydrogen bonding in the transition state of the $k'_1 - k'_{-1}$ step, one expects this hydrogen bonding to become stronger as BH becomes more acidic. This fact should be reflected in a Brønsted $\alpha > 0$ (or $\beta < 1$). Typical $\alpha$ values for preassociation mechanisms with hydrogen bonding range from 0.06[9] to 0.26,[10] with the majority being around 0.16–0.20.[9,11-14] Our $\alpha = 0.13$ is at the lower end of this range, as one would expect if the preassociation mechanism has to compete with the trapping mechanism for which $\alpha \approx 0$.

(6) (a) Millot, F.; Terrier, F. *Bull. Soc. Chim. Fr.* **1971**, 3897. (b) Terrier, F.; Millot, F.; Morel, J. *J. Org. Chem.* **1976**, *41*, 3892.
(7) Eigen, M. *Angew. Chem., Int. Ed. Engl.* **1964**, *3*, 1.
(8) Ahrens, M.-L.; Maass, G. *Angew. Chem., Int. Ed. Engl.* **1968**, *7*, 818.
(9) Abrams, W. R.; Kallen, R. G. *J. Am. Chem. Soc.* **1976**, *98*, 7777.
(10) Gilbert, H. F.; Jencks, W. P. *J. Am. Chem. Soc.* **1977**, *99*, 7931.
(11) Sayer, J. M.; Jencks, W. P. *J. Am. Chem. Soc.* **1973**, *95*, 5637.
(12) Kresge, A. J.; Tang, Y. C. *J. Chem. Soc., Chem. Commun.* **1980**, 309.
(13) Jencks, W. P.; Cox, M. M. *J. Am. Chem. Soc.* **1981**, *103*, 572.
(14) Bernasconi, C. F.; Leonarduzzi, G. D. *J. Am. Chem. Soc.* **1982**, *104*, 5143.

**Table VI.** Analysis of Results for the Trapping Mechanism at High Buffer Concentrations after Subtracting Contribution by the Preassociation Mechanism

| | $ClCH_2COOH$ | $CH_3OCH_2COOH$ |
|---|---|---|
| $k_1/k_{-p}^{BH}$, M[a] | 0.249 ± 0.033 | 0.267 ± 0.021 |
| $\tau_{hi,trap}^{-1}$, $s^{-1}$ [a] | 1130 ± 100 | 1020 ± 40 |
| $k_1$, $s^{-1}$ [b] | (2.49 ± 0.33) × $10^9$ | (2.67 ± 0.21) × $10^9$ |
| $k_1K_a^{OH}$, M $s^{-1}$ [c] | (7.02 ± 0.70) × $10^{-2}$ | |
| $pK_a^{OH}$ [d] | 10.55 ± 0.14 | 10.58 ± 0.11 |
| $k_{-1}$, $s^{-1}$ [e] | | (9.40 ± 0.24) × $10^2$ |
| $K_1$ [f] | (2.65 ± 0.40) × $10^6$ | (2.84 ± 0.28) × $10^6$ |
| $pK_o$ [g] | 4.13 ± 0.09 | |

[a] From plots of $\tau_{trap}$ vs $[BH]^{-1}$ according to eq 12. [b] Calculated from $k_1/k_{-p}^{BH}$ with $k_{-p}^{BH} = 10^{10}$ $M^{-1}$ $s^{-1}$. [c] From chloroacetate data where $K_a^{OH}K_1/a_{H^+} = 0.468$, $K_a^{OH}k_1/a_{H^+} = \tau_{hi}^{-1}/3.14$ and hence $K_a^{OH}k_1 = a_{H^+}\tau_{hi}^{-1}/3.14$. [d] From $k_1K_a^{OH}$ and $k_1$ above. [e] From methoxyacetate data where $K_a^{OH}K_1/a_{H^+} = 0.085$ and hence $k_{-1} = \tau_{hi}^{-1}/1.085$. [f] From $k_1/k_{-1}$. [g] $K_o = K_a^{OH}k_1/k_{-1}$.

A further consequence of the presence of the preassociation pathway is that there cannot be a complete leveling off for the plots of $\tau^{-1}$ vs buffer concentration. This means that $\tau_{hi}^{-1}$ ($k_{-p}^{BH}[BH] \gg k_1$) is given by

$$\tau_{hi}^{-1} = \frac{K_a^{OH}k_1}{a_{H^+}} + k_{-1} + \left(k_f^{pre}\frac{K_a^{BH}}{a_{H^+}} + k_r^{pre}\right)\frac{a_{H^+}}{K_a^{BH} + a_{H^+}}[BH]_o \quad (23)$$

Figure 5 shows the plot of the $\tau^{-1}$ values that were corrected for the medium effect ($\tau_{corr}^{-1}$, case III in Figure 3) for the example of the methoxyacetate acid buffer. Closer inspection of the plot suggests that the points at the five highest buffer concentrations may in face represent a straight line rather than the continuation of the leveling off. If this interpretation is adopted, the slope of this straight line must be given by eq 24 and its intercept by eq 25, while subtraction of the contribution of the preassociation mechanism from the overall $\tau_{corr}^{-1}$ is represented by eqs 26–28.

$$\text{slope} = \left(k_f^{pre}\frac{K_a^{BH}}{a_{H^+}} + k_r^{pre}\right)\frac{a_{H^+}}{K_a^{BH} + a_{H^+}} \quad (24)$$

$$\text{intercept} = \frac{K_a^{OH}k_1}{a_{H^+}} + k_{-1} \quad (25)$$

$$\tau_{corr}^{-1} - \tau_{pre}^{-1} = \tau_{trap}^{-1} \quad (26)$$

with

$$\tau_{pre}^{-1} = \text{slope}[BH]_o = \left(k_f^{pre}\frac{K_a^{BH}}{a_{H^+}} + k_r^{pre}\right)\frac{a_{H^+}}{K_a^{BH} + a_{H^+}}[BH]_o \quad (27)$$

$$\tau_{trap}^{-1} = \frac{k_1k_p}{k_{-p} + k_1} + \frac{k_{-1}k_{-p}}{k_{-p} + k_1} \quad (28)$$

The result of applying eq 26 is shown by the dashed curve in Figure 5. A similar analysis was performed for the data at high chloroacetic acid concentrations. The results of these analyses are presented in Table VI. The values obtained for $k_1/k_{-p}^{BH}$ and $\tau_{hi,trap}^{-1}$ are seen to be significantly lower than those in Table IV determined without taking into account the preassociation mechanism. This has the effect of reducing $k_1$ and $k_{-1}$ significantly, indicating that the preassociation mechanism makes a substantial contribution to the overall rate.

**Rate and Equilibrium Constants for Trapping Mechanism.** In Table VIIA we have summarized $k_1$, $k_{-1}$, $K_1$, and $pK_a^{OH}$ values obtained from the three methods of analysis described in the previous section. In those cases where the value of a parameter is somewhat different in the two buffers, an average value is given. The set of parameters calculated with corrections for both the medium effect and the contribution by the preassociation mechanism is believed to be the most reliable despite the uncertainties introduced by the correction procedures. This is because it takes into account all experimental observations, in particular the increase in $K_o$ with increasing buffer concentration (Table I) and the Brønsted $\alpha$ ($\beta$) values (Figure 4) that fall short of the required values of 0 (1.0) expected for a pure trapping mechanism.

**Table VII.** Summary of Rate and Equilibrium Constants

| | $k_1$, $s^{-1}$ | $k_{-1}$, $s^{-1}$ | $K_1$ | $pK_a^{OH}$ |
|---|---|---|---|---|
| A. 3,6-Dimethylcatechol 2,4,6-Trinitrophenyl Ether, 20 °C | | | | |
| without corrections | 9.22 × $10^9$ | 2.61 × $10^3$ | 3.53 × $10^6$ | 10.01 |
| with correction for medium effect | 1.28 × $10^{10}$ | 4.95 × $10^3$ | 2.59 × $10^6$ | 10.25 |
| with correction for medium effect and preassociation mechanism | 2.58 × $10^9$ | 9.40 × $10^2$ | 2.65 × $10^6$ | 10.56 |
| B. Catechol 2,4,6-Trinitrophenyl Ether, 25 °C | | | | |
| without corrections (ref 2) | 1.2 × $10^9$ | 1.0 × $10^4$ | 1.2 × $10^5$ | 10.34 |
| without corrections (new analysis) | 6.31 × $10^8$ | 3.43 × $10^3$ | 1.84 × $10^5$ | 10.55 |
| with correction for medium effect | ~6.5 × $10^8$ | ~3.5 × $10^3$ | ~1.9 × $10^5$ | ~10.55 |
| with correction for medium effect and preassociation mechanism | ~6.0 × $10^8$ | ~2.8 × $10^3$ | ~2.1 × $10^5$ | ~10.61 |
| C. 3,6-Dimethylcatechol/Catechol | | | | |
| with correction for medium effect and preassociation mechanism | ~4.3 | ~0.34 | ~12.6 | |

In retrospect it appears likely that the reaction of the parent catechol 2,4,6-trinitrophenyl ether is also subject to a similar medium effect, even though it affects the calculated kinetic and thermodynamic parameters only slightly because the highest buffer concentrations used in the previous study[2] are less than half of those used in the present one. Furthermore, on the basis of $k_{-p}^{BH}/K_1$ for chloroacetic and acetic acid, one calculates a Brønsted $\alpha \approx 0.08$, which also suggests a contribution by the preassociation mechanism, which, however, is smaller than that in the 3,6-dimethylcatechol 2,4,6-trinitrophenyl ether system ($\alpha$ = 0.13).

Table VIIB lists four sets of rate and equilibrium constants for the parent catechol 2,4,6-trinitrophenyl ether system. The first is the one reported in 1976[2] with no corrections applied. The second represents a recalculation of the first set based on a least-squares analysis of the data.[15] The third and fourth sets are based on the chloroacetic acid buffer and are corrected for the medium effect and for the medium effect plus preassociation mechanism, respectively. The parameters obtained in these two sets, and particularly the last one, are only approximate for two reasons. (1) No data were available to quantify the medium effect so it was assumed that it affects $K_o$ the same way as for the 3,6-dimethylcatechol 2,4,6-trinitrophenyl ether. (2) There is some uncertainty how to draw the line for the preassociation mechanism on the buffer plots of $\tau^{-1}$ vs $[BH]_o$.

Despite these uncertainties, the fourth set is considered to represent the most realistic rate and equilibrium constants, and hence a comparison of the rate and equilibrium constants for the two systems should be based on this fourth set and the third set for 3,6-dimethyl derivative. Note, however, that the qualitative conclusions to be reached are the same as long as the kinetic and thermodynamic parameters for the two systems are compared at the same level of analysis.

The comparison between the two systems yields the ratios summarized in Table VIIC. They indicate that the two methyl groups enhance $K_1$ by approximately 12.6-fold, $k_1$ by about 4.3-fold. Since $pK_a^{OH}$ is not significantly affected by the methyl groups, the increase in $K_1$ and $k_1$ cannot be attributed to an electronic effect but are consistent with the steric effect discussed in the introduction. However, the amount of acceleration is rather modest; even if one were to assume that after correction for the lower temperature (20 vs 25 °C) $k_1$ for the 3,6-dimethylcatechol 2,4,6-trinitrophenyl ether was 10–20-fold higher than for the

(15) The lack of a computer in 1976 precluded calculations by least-squares analysis.

**Table VIII.** Kinetic Parameters for the Preassociation Mechanism and Relative Contribution of Preassociation and Trapping Mechanisms

| | 3,6-dimethylcatechol 2,4,6-trinitrophenyl ether | | catechol 2,4,6-trinitrophenyl ether: $ClCH_2COOH$ |
|---|---|---|---|
| | $CH_3OCH_2COOH$ | $ClCH_2COOH$ | |
| $k_f^{pre} = K_aK_bk'_1$, $M^{-1}$ $s^{-1}$ [a] | (5.32 ± 0.5) × $10^3$ | (1.05 ± 0.08) × $10^3$ | (1.78 ± 0.36) × $10^2$ |
| $k_r^{pre} = K_{assoc}k'_{-1}$, $M^{-1}$ $s^{-1}$ [a] | (1.61 ± 0.15) × $10^3$ | (2.25 ± 0.20) × $10^3$ | (5.9 ± 1.2) × $10^3$ |
| $k_f^{trap} = k_p^B = K_aK_bk_c$, $M^{-1}$ $s^{-1}$ [b] | (8.14 ± 1.0) × $10^3$ | (1.26 ± 0.10) × $10^3$ | (1.0 ± 0.2) × $10^3$ |
| $k_r^{trap} = k_{-p}^{BH}/K_1 = k_{-c}/K_1$, $M^{-1}$ $s^{-1}$ [b] | (2.46 ± 0.30) × $10^3$ | (2.68 ± 0.23) × $10^3$ | (3.4 ± 0.7) × $10^4$ |
| $k_f^{pre}/k_f^{trap} = k'_1/k_c$ | 0.65 ± 0.13 | 0.83 ± 0.19 | 0.18 ± 0.07 |

[a] From eq 24 and the relation $k_f/k_r = K_o/K_a^{BH}$, as $k_f^{pre}$ = slope $[(K_a^{BH} + a_{H^+})/a_{H^+}][(K_a^{BH}/a_{H^+}) + (K_a^{BH}/K_o)]^{-1}$ and $k_r^{pre}$ = slope $[(K_a^{BH} + a_{H^+})/a_{H^+}][(K_o/a_{H^+}) + 1]^{-1}$. [b] $k_f^{trap}$ and $k_r^{trap}$ obtained in a similar way as $k_f^{pre}$ and $k_r^{pre}$, with "slope" being the difference in the observed slope at low buffer concentrations and the slope from eq 24.

parent catechol derivative, this rate increase still falls far short of the dramatic accelerations (~500000-fold) observed by Bunnett and Okamoto in the Smiles rearrangement shown in eq 4. In the absence of more systematic studies, it is difficult to pinpoint the reason for this large difference in the response to the introduction of the methyl groups in the two systems. One obvious possibility is that the C–S bond lengths in **4** and possibly the dihedral C–S bond angle at sulfur are different enough from the C–O bond lengths and the dihedral C–O bond angles at oxygen to have a profound effect on the reactivity difference between the respective parent and methyl derivatives. As discussed in a recent paper by Houk[16] the relation between reactivity and proximity in intramolecular reactions is not a simple one.

A comparison of the $pK_a^{OH}$ values shows them to be nearly the same (~10.61 for the catechol 2,4,6-trinitrophenyl ether, 10.56 for the 3,6-dimethyl derivative). This is consistent with the near sameness of the $pK_a$ values of catechol (10.64 ± 0.02) and 3,6-dimethylcatechol (10.68 ± 0.02) in the same solvent (see the Experimental Section). It also seems reasonable that the $pK_a^{OH}$ values are only slightly lower than the $pK_a$ values of catechol or 3,6-dimethylcatechol: the electron-withdrawing effect of the 2,4,6-trinitrophenyl group is counteracted by a statistical factor of two in favor of the unsubstituted catechols.

It should be noted that the $k_1$, $K_1$, and $pK_a^{OH}$ values obtained for the catechol 2,4,6-trinitrophenyl ether as well as for the 3,6-dimethyl derivative all depend on the assumption of $k_1^{BH} = 10^{10}$ $M^{-1}$ $s^{-1}$, as stated in the Results section. If $k_{-1}^{BH}$ were somewhat lower,[17] $k_1$ and $K_1$ would be reduced by the same amount while $K_a^{OH}$ would increase by the same factor. However, the *relative* values of these parameters for a given level of analysis (Tables IV, VI, and VII) and in comparing the two compounds would remain the same and so would all the conclusions drawn above.

**Preassociation Mechanism.** The kinetic parameters referring to the preassociation mechanism are summarized in Table VIII. The table also includes the corresponding parameters for the trapping mechanism at low buffer concentrations from which the relative contribution of the two mechanisms can be deduced. The following points are to be noted.[19]

(1) Even though the experimental error in the various kinetic parameters is too large for a determination of meaningful Brønsted coefficients, the qualitative picture that emerges from a comparison between methoxyacetic and chloroacetic acid is reasonable. Thus $k_r^{trap} = k_{-p}^{BH}/K_1$ is now within experimental error the same for the two buffers, implying $\alpha \approx 0$ as expected for a diffusion controlled reaction, while $k_r^{pre}$ shows a substantial dependence on the acid, implying a Brønsted $\alpha$ around 0.17 ± 0.09 for the preassociation pathway.

(2) The relative contribution by the pressociation mechanism increases with the acidity of the buffer as seen from $k_f^{pre}/k_f^{trap}$ ratios (note that $k_r^{pre}/k_r^{trap} = k_f^{pre}/k_f^{trap}$). This is a consequence of the different Brønsted coefficients for the two mechanisms.

(3) The contribution by the preassociation mechanism in the reaction of the parent catechol 2,4,6-trinitrophenyl ether is much smaller ($k_f^{pre}/k_f^{trap} = k'_1/k_c = 0.18$) than in the reaction of the 3,6-dimethyl derivative with the same buffer (0.83). This is reasonable since $k'_1$, just as $k_1$, should be smaller for the parent compound while $k_c$ for the diffusional separation between $S^-$ and BH should be about the same for the two compounds. From the $k'_1/k_c$ ratios for the two compounds and assuming identical $k_c$ values, we calculate that $k'_1$ for the dimethyl derivative is about 4.6-fold higher than for the parent compound. This is close to the ratio of the $k_1$ values (~4.3, Table VII) and, within experimental error probably the same, again a reasonable result.

## Conclusions.

The recognition, initially by Jencks,[3,10,11,13] that the lifetime of intermediates (real or virtual) is one of the most important factors that determine the mechanism of reactions, has been a major advance in our understanding of chemical processes. Scheme I shows a common situation where the lifetime of an intermediate, $S^-$·HB in this case, is indeed the deciding factor. The scheme illustrates two limiting cases. If the lifetime of $S^-$·HB is long enough so that $S^-$ and HB have the time to diffuse apart before $S^-$·HB collapses to form $M^-$·HB (i.e., $k_c > k'_1$), the diffusional separation of $S^-$ and HB will have to occur and $M^-$ will be formed by the $k_1$ step. Because of the principle of microscopic reversibility, the reaction must choose the same pathway in the reverse direction ($k_{-1} \rightarrow k_{-c} \rightarrow k_{-b} \rightarrow k_{-a}$), a pathway called enforced trapping (of the intermediate $S^-$ by diffusional-controlled protonation). If, on the other hand, the $k'_1$ step is so fast that there is no time for diffusional separation of $S^-$·HB (i.e., $k_c < k'_1$), the reaction is forced to choose the pathway $S^-$·HB $\rightleftarrows$ $M^-$·HB $\rightleftarrows$ $M^-$ + HB, which is the enforced preassociation mechanism. The third limiting case would occur if $k'_1$ were $>10^{13}$ $s^{-1}$ so that $S^-$·HB could no longer be considered a real intermediate. In such a situation the reaction would have to proceed directly from SH·$B^-$ to $M^-$·HB without intermediate, a so-called enforced concerted pathway.

The present study shows that the spiro Meisenheimer complex formation from catechol 2,4,6-trinitrophenyl ether is at the borderline between the enforced trapping and enforced preassociation mechanism, but mostly (≈85%) on the side of the trapping mechanism. The introduction of methyl groups into the 3- and 6-positions of the catechol moiety increases $k'_1$ by about 4.6-fold, thereby bringing the contribution by the preassociation mechanism to nearly 50% of the reaction. To the best of our knowledge, this constitutes the first example of a nucleophilic reaction at an aromatic carbon that is shown to proceed by an enforced preassociation mechanism. Interestingly it is not the anionic $\sigma$-complex[20] that is the short-lived intermediate in this case, but its precursor.

## Experimental Section

**Materials.** 3,6-Dimethylcatechol 2,4,6-trinitrophenyl ether was obtained using a modification of the method of Drozd et al.[21] To a stirred solution of 0.011 mol of sodium methoxide in 15 mL of methanol was added 1.51 g (0.011 mol) of 3,6-dimethylcatechol,[22] followed by slow

(16) Dorigo, A. E.; Houk, K. N. *J. Am. Chem. Soc.* **1987**, *109*, 3698.
(17) In water at 20 °C, $k_{-1}^{BH} = 10^{10}$ $M^{-1}$ $s^{-1}$ seems a good assumption, based on $k = 1.1 \times 10^{10}$ $M^{-1}$ $s^{-1}$ for $Cl_2CHCOOH + AcO^- \rightarrow Cl_2CHCOO^- + AcOH$.[18] In 50% $Me_2SO$ the higher viscosity may slightly reduce this value.
(18) Ahrens, M. L.; Maass, G. *Angew. Chem., Int. Ed. Engl.* **1968**, *7*, 818.
(19) In contrast to the results summarized in Tables IV, VI, and VII, none of the quantities in Table VIII depend on an assumed value for $k_{-1}^{BH}$.
(20) (a) Terrier, F. *Chem. Rev.* **1982**, *82*, 77. (b) Buncel, E.; Crampton, M. R.; Strauss, M. J.; Terrier, F. *Electron Deficient Aromatic- and Hetero-aromatic-Base Interactions*; Elsevier: Amsterdam, 1984.
(21) Drozd, V. N.; Knyazev, V. N.; Klimov, A. A. *Zh. Org. Khim.* **1974**, *10*, 826.
(22) (a) Fields, D. L.; Miller, J. B.; Reynolds, D. D. *J. Org. Chem.* **1964**, *29*, 2640. (b) Caldwell, W. T.; Thompson, T. R. *J. Am. Chem. Soc.* **1939**, *61*, 2354.

addition under $N_2$ of 2.72 g (0.011 mol) of picryl chloride in 70 mL of dry DMSO at ambient temperature. After 4 days, workup was performed by addition of an equal volume of ice/water, acidification to pH 2 with concentrated HCl, and filtration of the resultant precipitate. Recrystallization from water was performed by addition of the precipitate to 200 mL of water, followed by sufficient 1 M KOH to convert the ether to the anionic $\sigma$ complex (shown by a dark red color). An insoluble residue was removed by filtration. Acidification of the filtrate with concentrated HCl regenerated the ether (disappearance of the dark red color), followed by formation of a light yellow precipitate. Filtration and recrystallization from acidic ethanol/water yielded ~0.77 g (20% yield) of the ether: mp 139.5–141 °C; MS, *m/e* 349 (calcd for $C_{14}H_{11}O_8N_3$ *m/e* 349.25); $^1$H NMR (60 MHz, $CDCl_3$) $\delta$ 2.17–2.25 (2 s, 6 H, Ar $CH_3$), 4.74 (br s, 1 H, Ar OH), 6.64–6.97 (dd, 2 H, $J$ = 12 Hz, Ar H (catechol)), 8.80 (s, 2 H, Ar H (trinitrophenyl)).

Buffer materials were commercially available analytical reagent grade. Chloroacetic acid was recrystallized from hexanes before use. Dichloroacetic and methoxyacetic acids were vacuum-distilled before use. Typically, individual buffer solutions were prepared by diluting a concentrated stock buffer solution ($\mu$ = 0.5) with a 0.5 M KCl diluent solution. Substrate stock solutions were made as 0.05 M in dry DMSO prior to use. Catechol and 3,6-dimethylcatechol were purified by successive resublimations under vacuum, mp 102.5–104 and 100–101 °C, respectively.

**Equilibrium and Kinetic Measurements.** All equilibrium and kinetic measurements were performed at 20 °C in 50% DMSO/$H_2O$ (v/v), at ionic strength $\mu$ = 0.5 M, maintained with KCl.

Spectra and equilibrium measurements were taken on a Perkin-Elmer 559A spectrophotometer thermostatted to 20.0 ± 0.1 °C; pH measurements were performed with an Orion 611 pH meter with a Beckman 39402 reference electrode and a Corning 476022 glass electrode, calibrated at 20 °C with Hallé buffers.[23] The pseudo-equilibrium constant ($pK_o$) was determined spectrophotometrically ($\lambda_{max}$ = 472 nm, $\epsilon_M$ = 1.85 × $10^4$ $M^{-1}$ $cm^{-1}$ (complex), $\epsilon_{SH}$ = 80 $M^{-1}$ $cm^{-1}$ (substrate)) in chloroacetate buffers at constant 0.1 M free buffer, and $pK_o$ was obtained from eq 29. Measurements of $K_o$ as a function of buffer concentration (Table I) were performed in the same solutions as used for the temperature-jump experiments; constant buffer pH was obtained by adjustment with concentrated KOH or HCl.

$$pK_o = pH + \log \frac{\epsilon_M[SH]_o - OD_{obsd}}{OD_{obsd} - \epsilon_{SH}[SH]_o} \quad (29)$$

The $pK_a$ values of catechol and 3,6-dimethylcatechol were determined potentiometrically from half-neutralized solutions; solvents were purged with $N_2$ prior to use to retard oxidation of the catechols.

The kinetic experiments at low buffer concentrations were performed in a Durrum–Gibson stopped-flow spectrophotometer with automated data collection.[24] Associated pH measurements were performed by the mock-mixing method. The kinetics at high buffer concentrations were measured in a Messanlagen temperature-jump transient spectrophotometer. Observed pseudo-first-order rate constants were obtained from photographs as the average of five or more shots. Temperature-jump reaction solutions were equilibrated to 16.0 ± 0.2 °C prior to a discharge of 25 kV (calibrated to produce a jump of 4 °C in 50% DMSO/$H_2O$). These solutions were previously deaerated by the brief application of vacuum and sonication to reduce cavitation effects. Final substrate concentration for the kinetic work was $\leq 5 \times 10^{-5}$ M.

(23) Hallé, J.-C.; Gaboriaud, R.; Schaal, R. *Bull. Soc. Chim. Fr.* **1969**, 1851.

(24) Software developed by Dr. F. A. Brand.

**Corrections for Medium Effects.** From eq 15 and the relationship $k_f/k_r = K_o/a_{H^+}$, one obtains

$$k_f = \frac{1}{\tau}(1 + a_{H^+}/K_o)^{-1} \quad (30)$$

$$k_r = \frac{1}{\tau}(1 + K_o/a_{H^+})^{-1} \quad (31)$$

for the relative contributions of $k_f$ and $k_r$ to $\tau^{-1}$. At the pH values of the temperature-jump experiments we have

$$k_f = 0.068\tau^{-1} \qquad k_r = 0.932\tau^{-1} \quad (32)$$

in the methoxyacetic acid buffers,

$$k_f = 0.307\tau^{-1} \qquad k_r = 0.693\tau^{-1} \quad (33)$$

in the chloroacetic buffers.

At high buffer concentrations $K_o$ changes to $K'_o = \gamma K_o$, while $k_f$ changes to $k'_f$, $k_r$ to $k'_r$, and hence eq 15 becomes

$$\frac{1}{\tau'} = k'_f + k'_r \quad (34)$$

Case I: If the entire change in $K_o$ can be attributed to an increase in $k_f$, we have $k'_f = \gamma k_f$, $k'_r = k_r$, and

$$\frac{1}{\tau'} = \gamma k_f + k_r \quad (35)$$

Case II: If the entire change in $K_o$ can be attributed to a decrease in $k_r$, we have $k'_f = k_f$, $k'_r = \gamma^{-1}k_r$, and

$$\frac{1}{\tau'} = k_f + \gamma^{-1}k_r \quad (36)$$

Case III: If the change in $K_o$ is equally distributed between $k_f$ and $k_r$, eq 34 becomes

$$\frac{1}{\tau'} = \gamma^{1/2}k_f + \gamma^{-1/2}k_r \quad (37)$$

Combining eq 32 (methoxyacetic acid) with eqs 35–37 yields eqs 38–40 for cases I–III, respectively, with $1/\tau_{extrap}$ referring to a $1/\tau$ value obtained by extrapolation from the buffer dependence at low concentrations; $1/\tau'$ for the chloroacetate acid buffers were obtained in a similar way by combining eq 33 with eq 35–37, respectively.

$$\frac{1}{\tau'} = Z\frac{1}{\tau_{extrap}} \qquad Z = 0.068\gamma + 0.932 \quad (38)$$

$$\frac{1}{\tau'} = Z\frac{1}{\tau_{extrap}} \qquad Z = 0.068 + 0.932\gamma^{-1} \quad (39)$$

$$\frac{1}{\tau'} = Z\frac{1}{\tau_{extrap}} \qquad Z = 0.068\gamma^{1/2} + 0.932\gamma^{-1/2} \quad (40)$$

The corrected values for $1/\tau$ plotted in Figures 2 and 3 were then obtained as

$$\frac{1}{\tau_{corr}} = \frac{1}{Z\tau_{obsd}} \quad (41)$$

**Supplementary Material Available:** Kinetic data in acetate, methoxyacetate, chloroacetate, and dichloroacetate buffers, Tables S1–S5 (8 pages). Ordering information is given on any current masthead page.